

# Chapter 3

## Apparatus

### 3.1 CESR Storage Ring

CESR, the Cornell Electron Storage Ring, was built from 1977 to 1979. It is located in a tunnel 768 meters in circumference under an athletic field on the Cornell University campus in Ithaca, New York. Its main objective is to accelerate particles to the desired energy, to store them for collisions, and to focus these tiny beams to produce as high a luminosity as possible. The CESR ring is shown in Fig 3.1.

CESR operation contains three parts:

- electron and positron beam production from Linear Accelerator (Linac).
- synchrotron acceleration.
- CESR storage ring.

CESR is processed as follows: injected electron and positron beams produced in the Linac will be directed to the synchrotron to be accelerated to the desired energy, then guided into

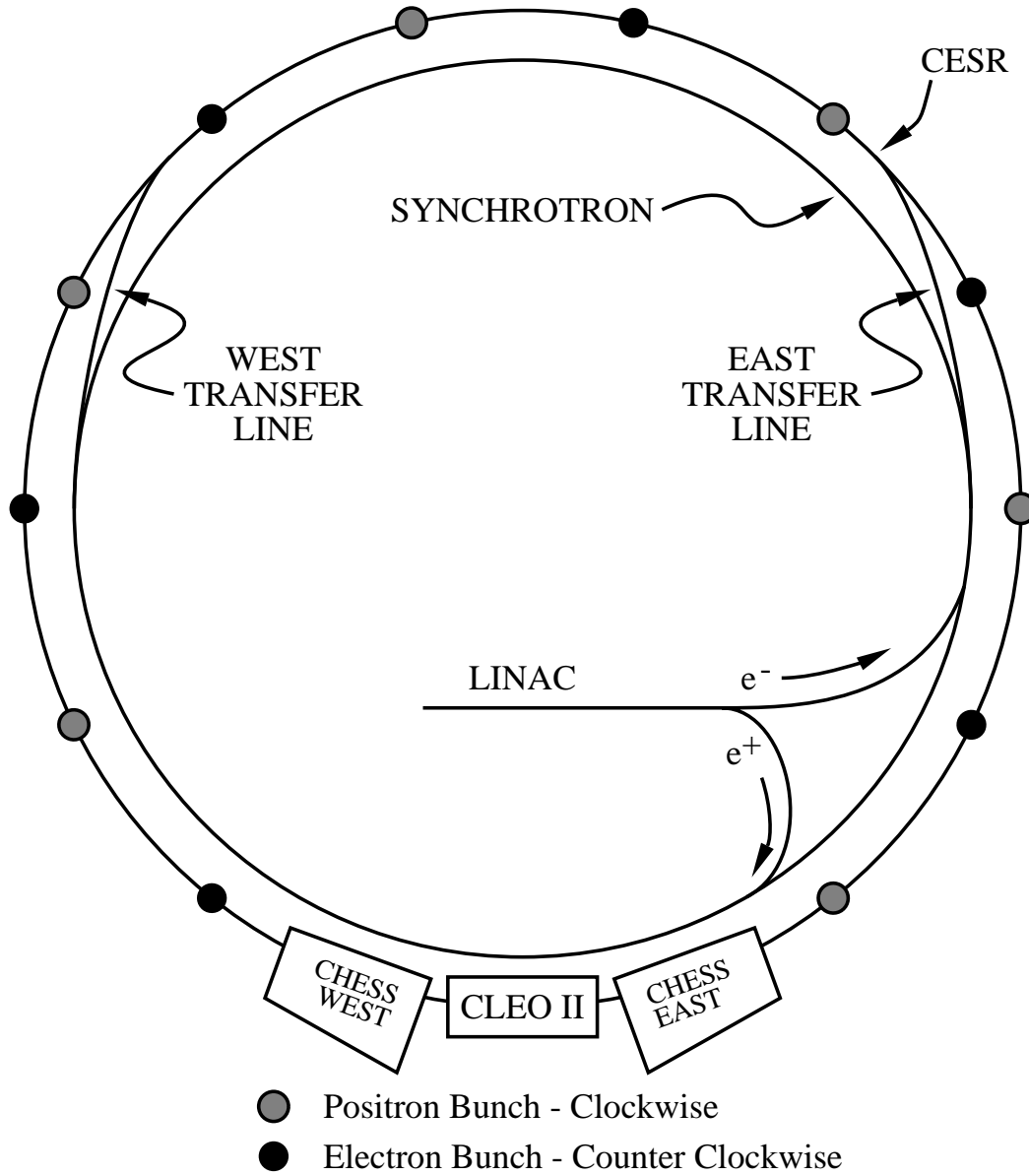


Figure 3.1: The CESR Accelerator

the storage ring to accumulate electrons and positrons in opposing directions. The two beams collide at the center of the CLEO detector.

### **3.1.1 Production of Electron and Positron Beam**

The electron beam is produced by applying high voltage at the back end of heated Linac to create the electron beam. The electrons gain energy to about 200 MeV while accelerating in the 30 meter long vacuum tube before being projected into the synchrotron ring.

Some of the electrons in the Linac will be directed to bombard a tungsten target to produce electron-positron pairs. The positrons will be accelerated and then injected into synchrotron ring in the direction opposite to the electron.

### **3.1.2 Beam in Synchrotron**

There are magnets in the synchrotron ring. Because electrons and positrons have the same mass with opposite charge, they will travel in opposite directions when they are accelerated in the synchrotron. They reach an energy of about 5 GeV, about 4000 turns in the synchrotron. This energy for electrons and positrons corresponds to 99.999995% of the speed of light.

While electrons and positrons circulate, they lose on average about 1 MeV per turn by emitting X-ray radiation. The radio frequency cavities, RF, add this energy back on every loop.

### **3.1.3 CESR for Collision at CLEO**

When electrons and positrons reach the desired energy, they will experience a “kick” to push them into the CESR ring for collision at the center of CLEO detector. Those electrons

and positrons in the synchrotron do not come continuously but travel in bunches. Each bunch has as many as  $1.5 \times 10^{11}$  particles in it and its size is about 1.1 mm wide, 0.1 mm high and about 1.0 cm long. The bunches circulate at about 396 kHz in the ring.

Accelerator performance is measured by luminosity. The formula to calculate luminosity is:

$$L = fn \frac{N_{e^+} N_{e^-}}{A} \quad (3.1)$$

where,

- f: revolution frequency.
- n: number of bunches of each particle type.
- $N_{e^-}$ : number of electrons in each bunch.
- $N_{e^+}$ : number of positrons in each bunch.
- A: cross-section area of the beam.

The luminosity of CESR has achieved a world record of  $4.0 \times 10^{32} \text{ cm}^{-2} \text{ s}^{-1}$ . The CESR luminosity history can be seen in Figure 3.2.

## 3.2 CLEO II Detector

The data for this dissertation was collected at the CLEO II detector. The CLEO II detector was operated in the period of 1989-1995, and later was replaced by the CLEO II.5 detector, which substituted the innermost drift chamber with a silicon vertex detector. The data collected from the CLEO II.5 detector is not included in our analysis. Figure 3.3 and

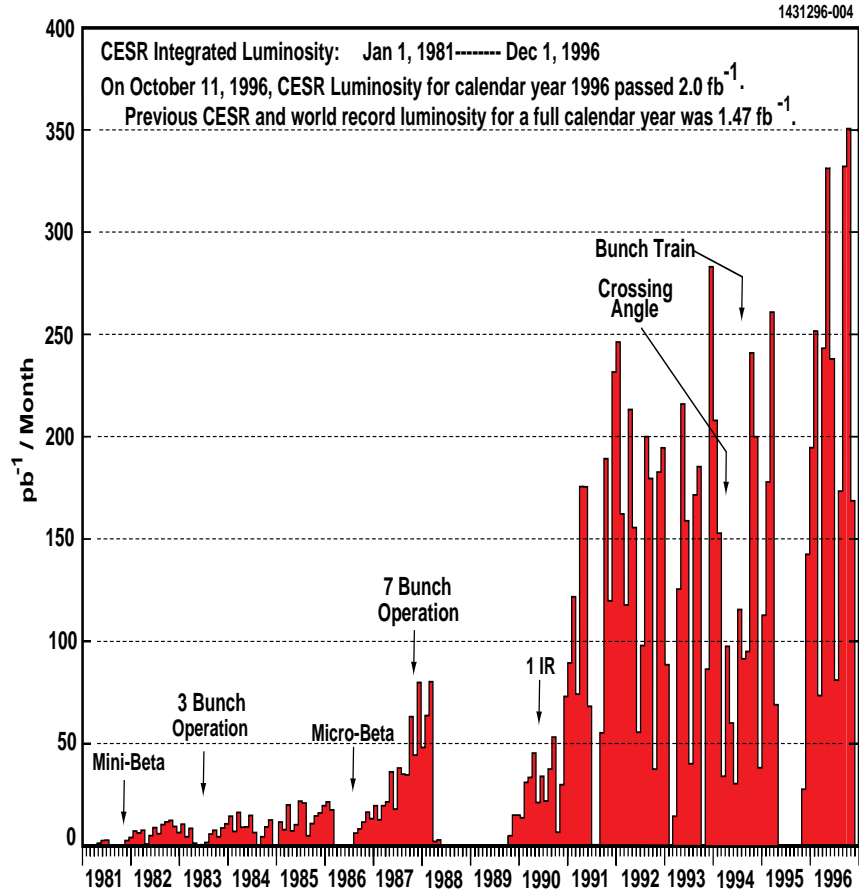


Figure 3.2: The CESR Luminosity history from 1981-1996. Originally, CESR was running on one bunch of each species. It then increased to three bunches, seven bunches, nine bunches and finally to nine trains with two bunches in each train. A major shut down had taken place in 1988-1989 to install the CLEO II detector. After that shutdown, CESR also only collided beams in one detector instead of two (CLEO and CUSB).

Figure 3.4 shows the cross section of the side view and the end view of CLEO-II detector, respectively.

The CLEO II detector is a  $4\pi$  detector, which means it covers almost all the solid angle. The entire detector is about 6.5 m tall, 6.5 m wide, and 5.8 m long and weighs about 1000 tons. Its major upgrades in 1989 included a smaller radius beam pipe, a straw tube tracking chamber inside the vertex detector, a time of flight system, a large radius of superconducting solenoid and a cesium iodide (CsI) crystal calorimeter. A detailed description of the CLEO II detector can be found at [32].

The CLEO II detector is composed of several components. A particle produced at the center of the detector, where the electron-positron beam collision takes place, will first pass through beam pipe (BP), then the central detector region (CD) which is composed of several different parts of a drift chamber. Outside the central detector is the Time of Flight detector (TF).

Both neutral and charged particles that pass through the Time of Flight detector enter the calorimeter (CC). The calorimeter gives a very accurate measurement of the energy and position through the “shower” that particle has left behind. Electrons and photons lose almost all of their energy in these showers. Some other particles like muon lose very little. The comparison between the energy of the shower and the momentum of the particle allows one to identify the electron candidates.

Outside the calorimeter sits the Superconducting Solenoid Coil that generates a uniform magnetic field of 1.5 Tesla pointing along the beam axis. A charged particle with momentum component perpendicular to the beam will be bent by the magnetic field. The curvature of the track can also provide information on the momentum of the charged particle.

The muon chamber sits outside the Superconducting Solenoid. The muon itself interacts rather weakly with the various detectors located inside muon chamber. Muon candidates

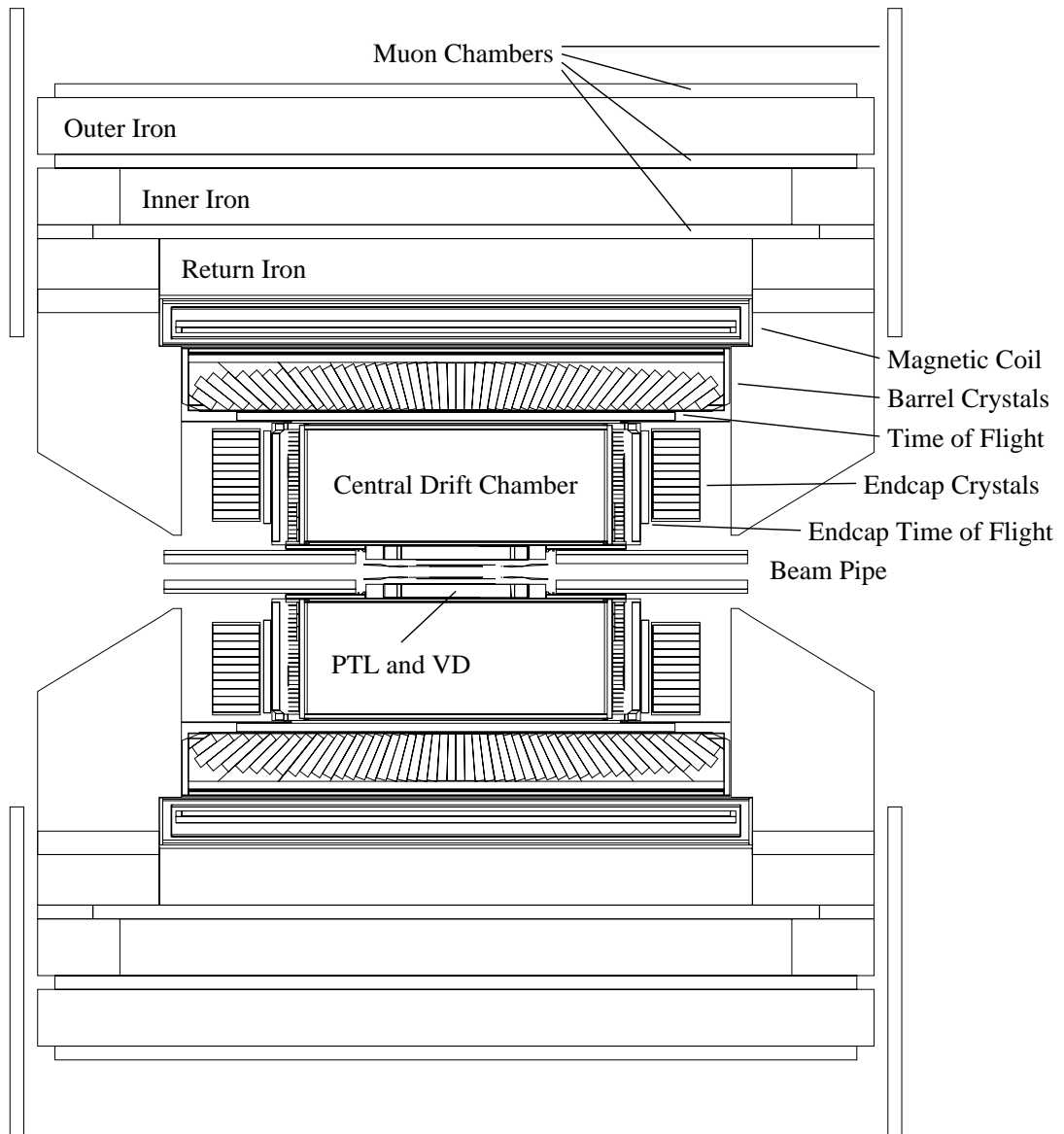


Figure 3.3: The CLEO II Detector Side-View

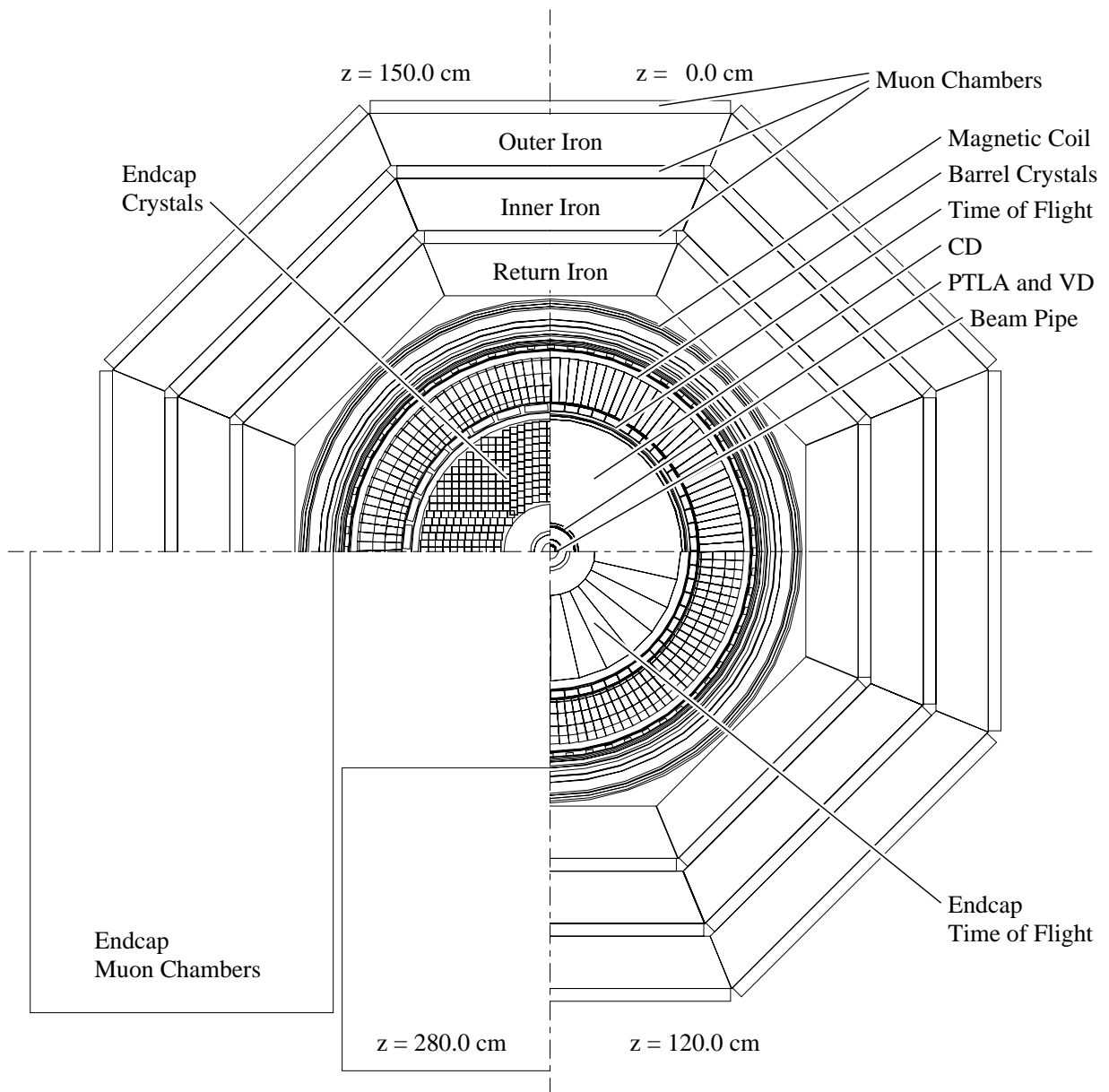


Figure 3.4: The CLEO II end view, four quarters at different  $z$



are thus identified as any charged track that makes it through to hit the muon chamber. Charged hadronic particles that were not absorbed by the iron will leave traces in the muon chamber, thus creating the “fake” muon candidates. The iron placed before the muon chamber allows only muons with momentum greater than 0.8 GeV/c to leave their traces in the first superlayer of the muon chamber.

We use a cylindrical coordinate system to describe the CLEO II detector, where the  $z$  axis is parallel to the beam pipe. The  $r - \phi$  plane is the plane transverse to the beam axis.

### 3.2.1 Beam Pipe

The beam pipe is a thin-walled beryllium pipe that separates the vacuum of the storage ring from the detector. This beryllium pipe is of thickness of 0.5 mm with length of 33 cm and radius of 3.5 cm. A silver layer of 20 microns and a nickel layer less than 1 microns are plated inside the beam pipe to reduce the background from synchrotron radiation.

### 3.2.2 Central Detector

The central detector is composed of three smaller drift chambers: the precision tracking layer (PT), the vertex detector (VD) and the main drift chamber (DR).

When a charged particle passes through the gas, it leaves a trace of ionized gas through ionization energy loss. The ionized particles produced by this process will be collected at the adjacent sense or field wire to enable us to register the location of the charged particles. These three concentric chambers (PT, VD and DR) run parallel, or nearly parallel, to the beam pipe, allowing excellent tracking reconstruction in the  $r - \phi$  plane.

## **Precision Tracking Layer (PT)**

The PT extends from -22.5 cm to 22.5 cm in the z direction, and from 4.7 cm to 7.2 cm in the radial direction. It consists of six concentric rings of 64 aluminized mylar tubes in each layer. Each tube serves as a cathode with a wire strung down the middle as an anode. The tubes have diameters between 2.2 and 3.5 mm. The PT chamber is operated at a high voltage of about 1500 V for each tube.

There were different gases used in the PT. Originally an equal mixture of Argon-Ethane was used as the gas, which resulted in a position resolution of approximately 100  $\mu m$ . In 1992, a new gas, DME (Dimethyl Ether), was used to substitute for the Argon-Ethane gas, improving the position resolution to 60  $\mu m$ .

## **Vertex Detector (VD)**

The VD extends from -35 cm to 35 cm in the z direction, and from 8.4 cm to 16.0 cm in the radial direction. The inner five layers consist of 64 cells each and the outer five layers of 96 cells. Gas in the VD is an equal mixture of Argon Ethane, with a higher pressure (20 psi) compared with PT, to reduce diffusion.

There are 800 sense wires for these 10 layers, with field wires forming hexagonal cells about them. Cathode strips were placed inside both the inner and outer radius walls of the VD. These strips are composed of 8  $\mu m$  of aluminum deposited on 75  $\mu m$  thick mylar, and serve to measure the z-position. Since anode wires are read out at both ends, a z position measurement can be achieved through the “charge division” method, which compares the relative amplitude of signal observed at opposite ends of each sense wire. Using this method, the z-position is measured with a resolution of 1.7 cm.

The Precision Tracking Chamber (PT) and the Vertex Detector (VD) are shown in Fig 3.5

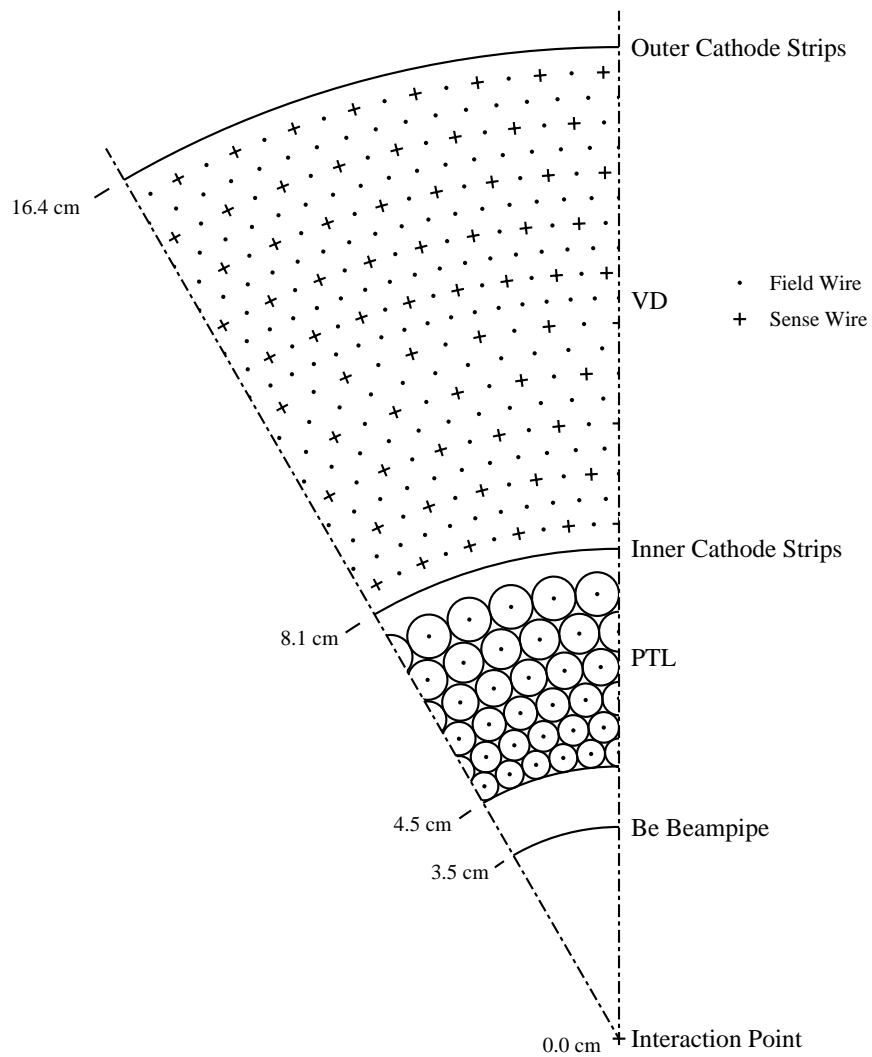


Figure 3.5: The CLEO II Precision Tracking Chamber and Vertex Detector

## Main Drift Chamber (DR)

The DR is located outside the VD, and extends from 17.5 cm to 95.0 cm in radius and from -94.5 cm to 94.5 cm in length. It consists of 51 layers, with 12240 sense wires and 36270 field wires. DR covers 94% of  $4\pi$  at the inner surface and 71% of  $4\pi$  at the outer surface. Figure 3.6 shows the picture of the CLEO II Drift Chamber (DR)

Among the 51 layers, 40 of them are the axial layers whose sense wire is pointing parallel to the beam. These 40 axial layers provide position measurements in the azimuthal direction.

Groups of three or five axial layers alternate with a “stereo layer” whose sense wires are about 5 degree to the beam axis. These “stereo layers” and the cathode strips in the inner and outer surfaces of the chamber provide measurements in the  $z$  direction. There are a total of 11 stereo layers in the main drift chamber.

Each cell is about 14 mm by 14 mm in size, with eight field wires surrounding a gold plated 20  $\mu\text{m}$  diameter tungsten sense wire. In the first 40 layers, we use aluminum for the field wires. For the remaining 11 layers, a copper-beryllium alloy is used.

The resolution of tracking system is measured to be

$$(\delta p_t/p_t)^2 = (0.0011p_t)^2 + (0.0067)^2 \quad (3.2)$$

where  $p_t$  is the transverse momentum in GeV/c. For  $p_t = 5.280$  GeV/c, the resolution,  $\delta p_t$ , is about 47 MeV/c. The angular resolution measured in  $e^+e^- \rightarrow \mu^+\mu^-$  events is found to be 1 mrad in  $\phi$  and 4 mrad in  $\theta$ . The spatial resolution is about 150  $\mu\text{m}$ .

The particle identification in this main drift chamber is realized by picking up the ionization energy collected at the sense wire. Particles with velocity,  $\beta = \frac{v}{c}$ , are characterized by their ionization energy loss per distance according to the following formula:

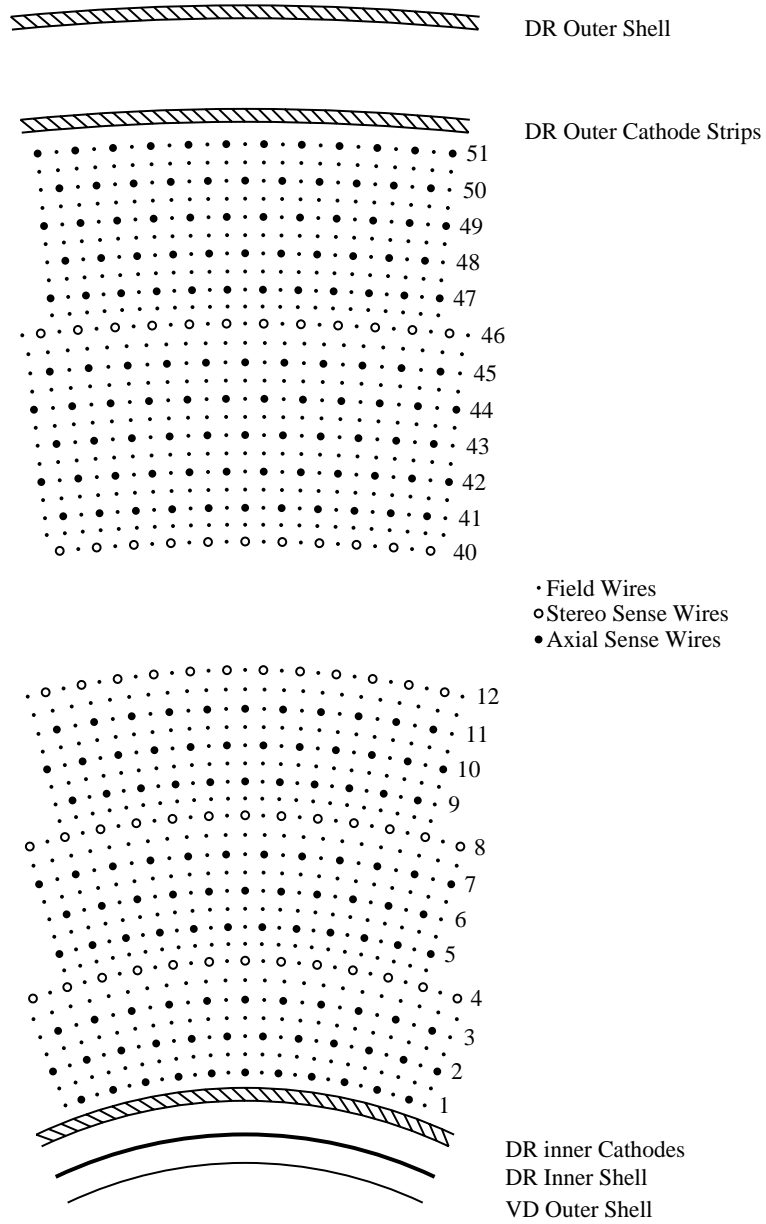


Figure 3.6: The CLEO II Drift Chamber

$$\frac{dE}{dX} = K \frac{Z}{A\beta^2} \left[ \frac{1}{2} - \ln \frac{2m_e\beta^2\gamma^2 T_{max}}{I^2} - \beta^2 - \frac{\delta}{2} \right] \quad (3.3)$$

Fig 3.7 is the diagram of the ionization energy loss for different particle species as a function of momentum.

### 3.2.3 Time of Flight Counter (TF)

Outside the DR is the TF system, which covers 97% of  $4\pi$  region by “barrel TF” counters and “endcap TF” counters. Barrel TF covers  $35^\circ - 145^\circ$  and endcap TF covers  $15^\circ - 35^\circ$  and  $145^\circ - 165^\circ$ , to cover both ends.

The barrel TF module is made of a scintillator, a lightguide and a photomultiplier tube. A charged particle passing through the plastic excites the organic molecules, which then emit ultraviolet light when they decay back to the ground state. Photons will bounce through internal reflection down the length of the scintillator into a plastic light guide that directs light into a photomultiplier glued at the end. There are 64 scintillators in the barrel TF, each is 279.4 cm long and about 10 cm wide. The CLEO II TF barrel system is shown in Figure 3.8.

For the endcap TF, we have 28 scintillators that are trapezoidal in shape. The photomultiplier is directly attached to the end of the scintillator. The endcap TF scintillator is about 4.8 cm thick. The endcap TF counter is shown in Figure 3.10.

The resolution of the TF detector ranges from 120 ps to 250 ps, with an average of 170 ps. The time of flight system determines the species of the charged particle by measuring the particle’s velocity, once the momentum is known from the curvature of the track within the tracking chambers. Figure 3.9 shows the TF  $1/\beta$  diagram for different particle species as a function of momentum, where  $\beta = v/c$ .

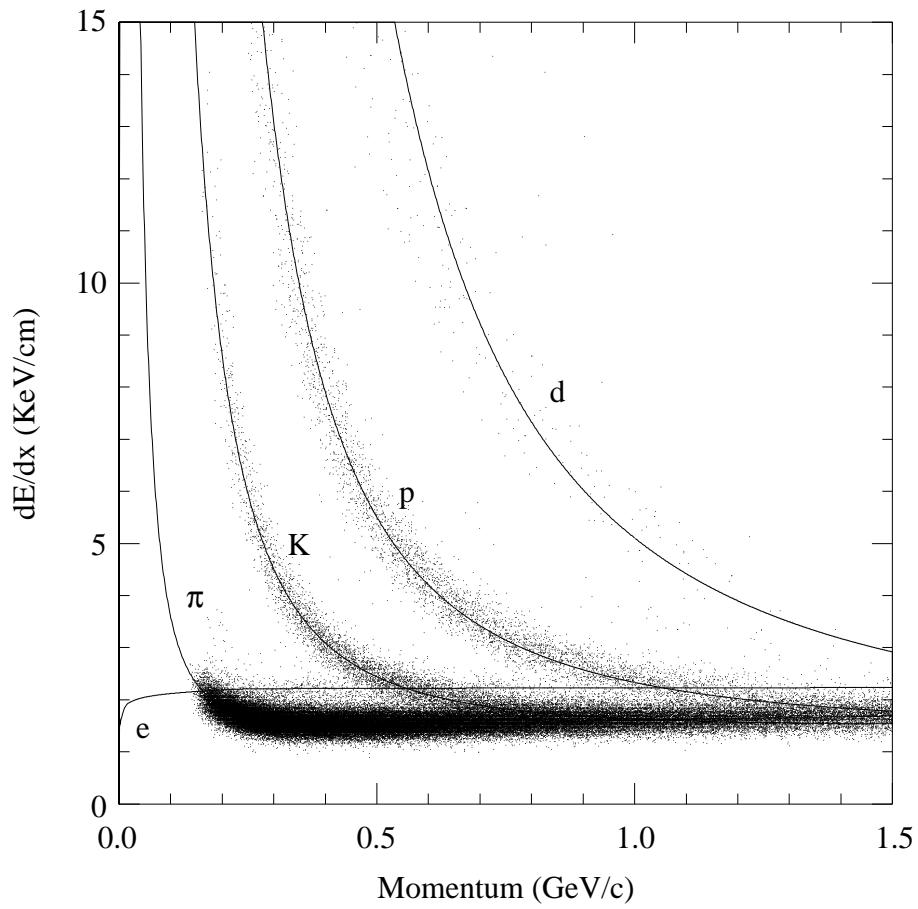


Figure 3.7: The Particle ionization energy loss with momentum

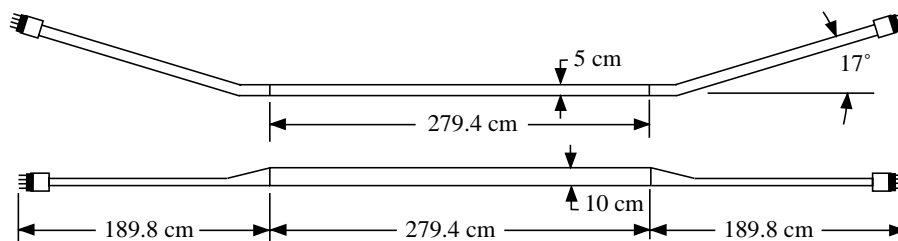


Figure 3.8: The CLEO II Barrel TF Counter

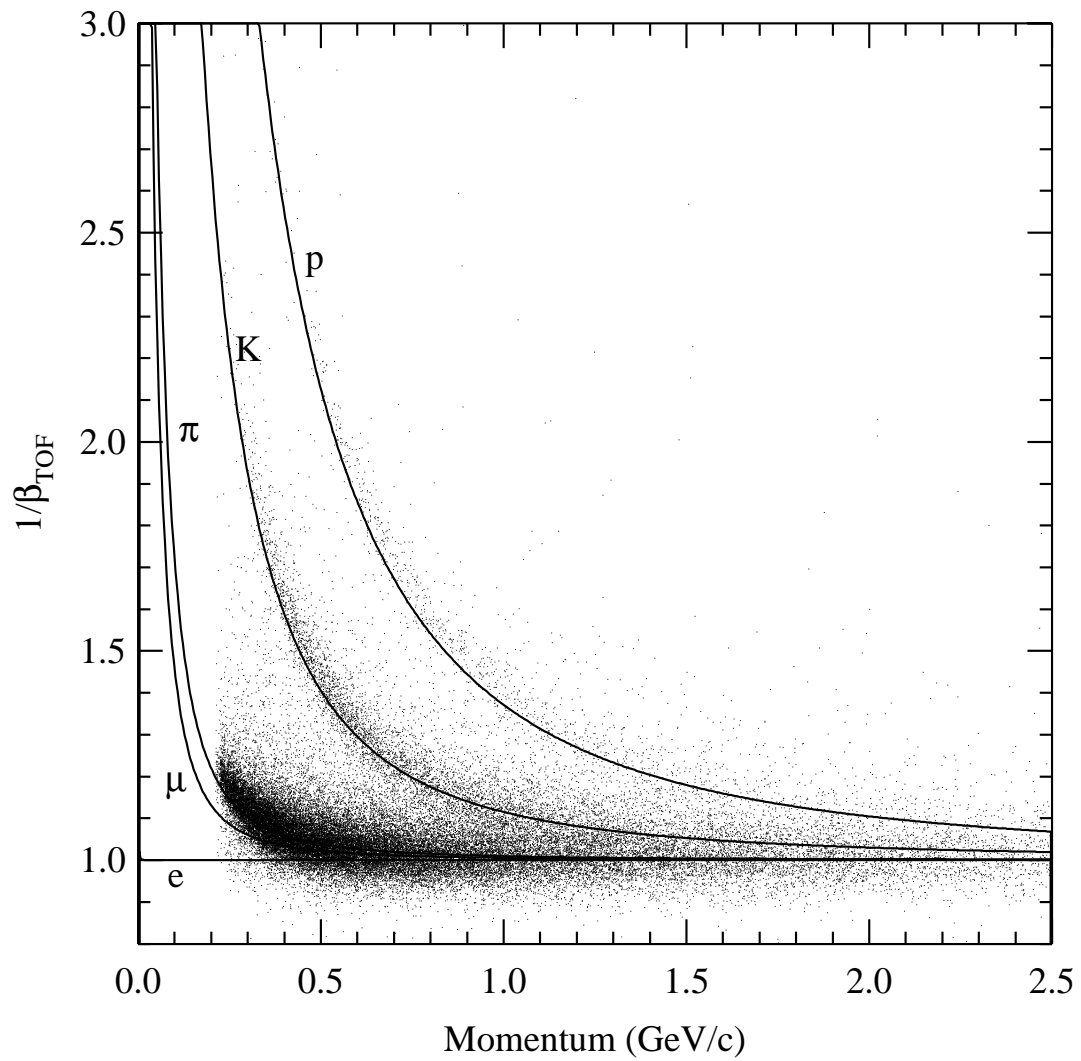


Figure 3.9: The CLEO II Time of Flight particle velocity with momentum



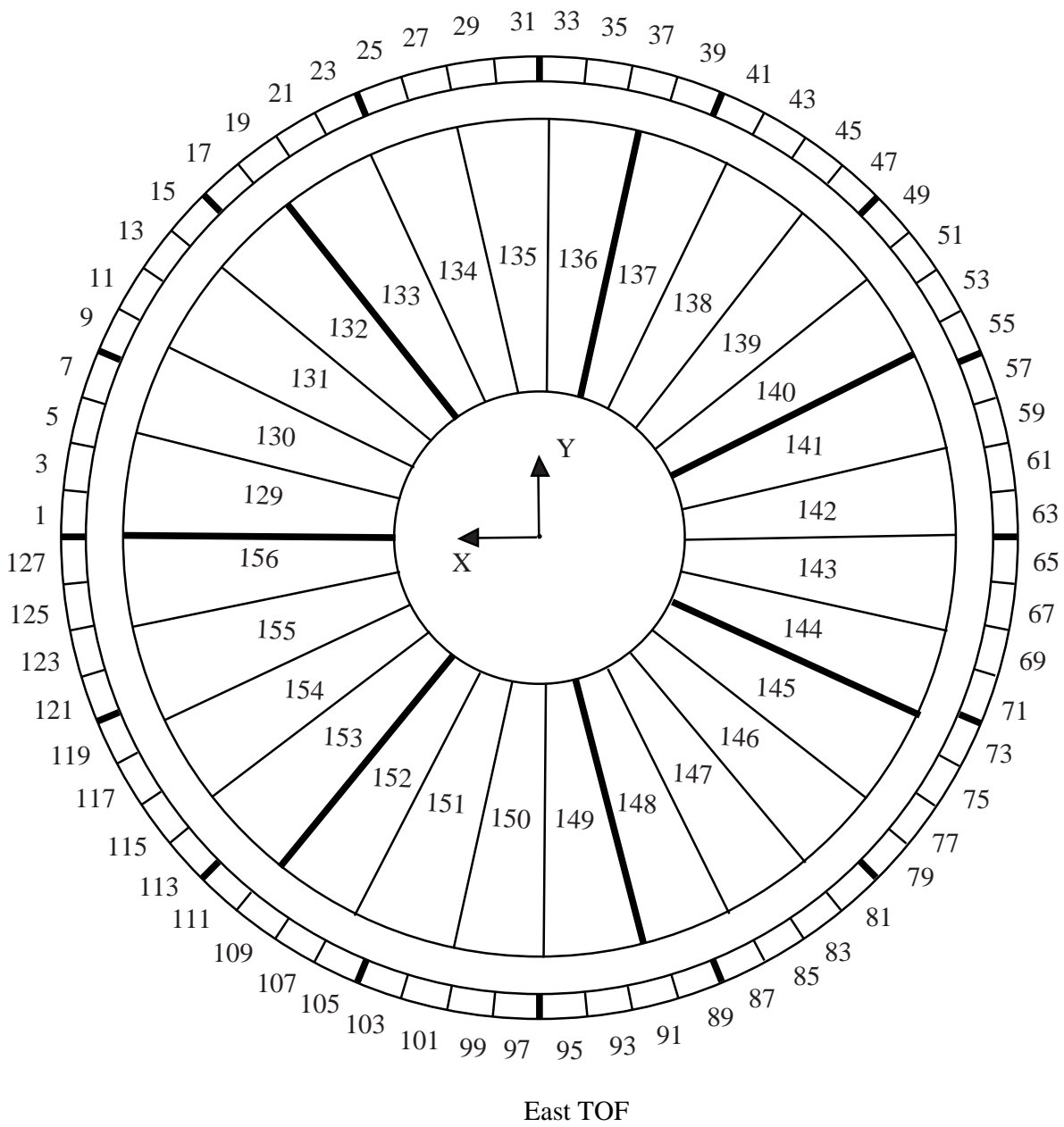


Figure 3.10: The CLEO II Endcap TOF Counter

### 3.2.4 Electromagnetic Calorimeter (CC)

Outside the TF counter is the Electromagnetic Calorimeter (CC). Like TF, it also consists of barrel and endcap regions. The CC is made of 7800 scintillating cesium iodide crystal blocks doped with thallium. Each crystal is about 5 cm square and 30 cm in length. The crystal end is pointed a few centimeters away from the interaction point to avoid showering photons slipping back through a crack. The 30 cm length of crystal is about 16 radiation length, to assure very little energy leaks out the back of the crystal. Through the readout of the pulse height, we can obtain the amount of energy deposited in the crystal. The CC contains 6144 crystals for the barrel region and 828 crystals on the endcaps.

Electrons and photons lose nearly all of their energy in CC, and the shower shape is very localized. Muons lose very little of their energy. Hadrons do not lose all of their energy either. Because secondary hadrons can be produced through nuclear interactions in the CC, we will have secondary hadron showers, which make the shower shape non-localized.

This Calorimeter has achieved very good resolution for photons. The energy resolution of photons is about 1.5% (2.6%) for photons with momentum of 5 GeV/c and 3.8% (5%) for photons with 100 MeV/c in momentum for the barrel (endcap). The spatial resolution of photons with momentum 5 GeV/c is about 3 mrad (9 mrad) and 11 mrad (19 mrad) of photons with momentum 100 MeV/c for the barrel (endcap) region. The excellent performance of the CLEO Crystal Calorimeter gives CLEO a great advantage in detecting neutral particles. For neutral pion decays to 2 photons, the energy resolution of  $\pi^0$  is about 5 MeV.

In this thesis, the usefulness of the calorimeter lies in its ability to identify the electrons. The ratio of  $E/p$ , the energy measured in the calorimeter and the momentum measured in the central detector tracking chambers, is a very powerful figure of merit for electron identification. An  $E/p$  close to 1 is consistent with an electron hypothesis since all of the electron's energy should be deposited in the calorimeter. Hadrons and muons have smaller

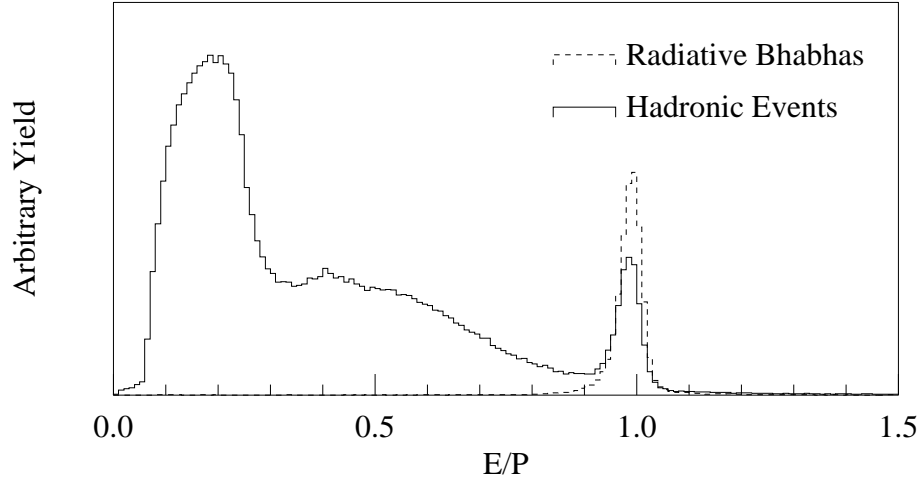


Figure 3.11: E/P yield for electrons from radiative Bhabha events compared to charged tracks in hadronic events in the momentum range 0.8 - 3.0 GeV/c at barrel region.

E/p. An example of E/p can be seen in Figure 3.11. This can be combined with other information from the calorimeter, and from the  $dE/dX$  measurements in the drift chamber to calculate the sum of the log likelihood ratio,  $L_e$ , for the track to be an electron. We define it to be:

$$L_e = \sum_i \ln(P_{ei}/P_{\neq ei}) \quad (3.4)$$

where  $P_{ei}$  is the probability that a track is an electron according to the  $i^{th}$  estimator, and  $P_{\neq ei}$  is the probability that the track is identified as  $\mu, K, p$  or  $\pi$ .

### 3.2.5 Superconducting Solenoid

The Superconducting Coil weighs about 30 tons and sits outside the CC. It produces a 1.5 Tesla field in the z direction. The coil consists of two layers, each with 650 turns of a superconducting cable made by Cu-Nb-Ti. Liquid helium is used to maintain the coil at a

temperature of 4 Kelvin. The 800000 kg steel yoke is used to shield magnetic flux for the outermost muon chamber.

### 3.2.6 Muon Chamber

The muon chamber is the outermost component of the CLEO II detector. The barrel muon counter covers the angular region  $45^{\circ} - 90^{\circ}$  and the endcap muon counter covers the angular region  $30^{\circ} - 45^{\circ}$ . The barrel muon counter is composed of eight octants of three layers of 30 cm thick steel interleaved with “superlayers”. These superlayers are composed of three single layers of proportional drift cells formed from extruded plastics, 5 m long and 8.3 cm wide. Hit position in  $\phi$  is measured by reading the anode wire, and z direction from the external copper strip. The Argon-Ethane gas recycled from the drift chamber flows through the muon counter.

In the barrel region, muons with momentum greater than 0.8 GeV/c can reach the first layer. To reach the second and third layers, muons need to have a momentum greater than 1.4 GeV/c and 1.8 GeV/c, respectively. The resolution of muon hit positions are determined by the error on the propagation of the track to the muon counters, the intrinsic resolution of the muon counters and multiple scattering in the material in front of the counters.

Fig 3.12 shows the cross section of a muon proportional chamber. We can see in Fig 3.13 the cross section of the superlayer chamber in the muon detector.

### 3.2.7 Trigger System

The crossing rate for the bunches of electrons and positrons in CESR is 2.7 MHz, while the rate of interesting events is only about 10 Hz. It is not possible to record the result of each beam crossing. CLEO II has three levels of triggers to select interesting events. Events

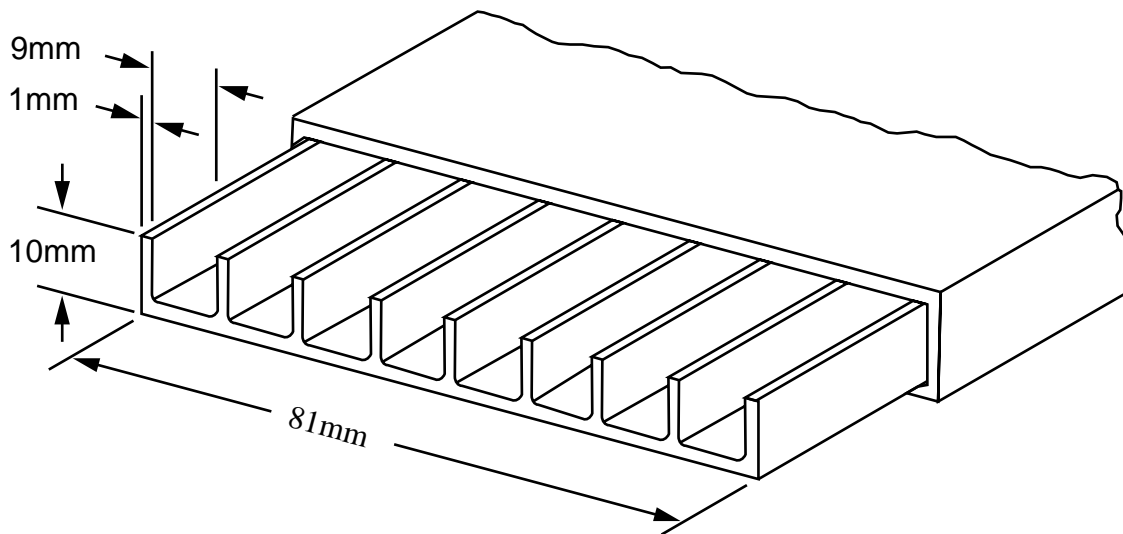


Figure 3.12: Cross Section of Muon Proportional Chamber

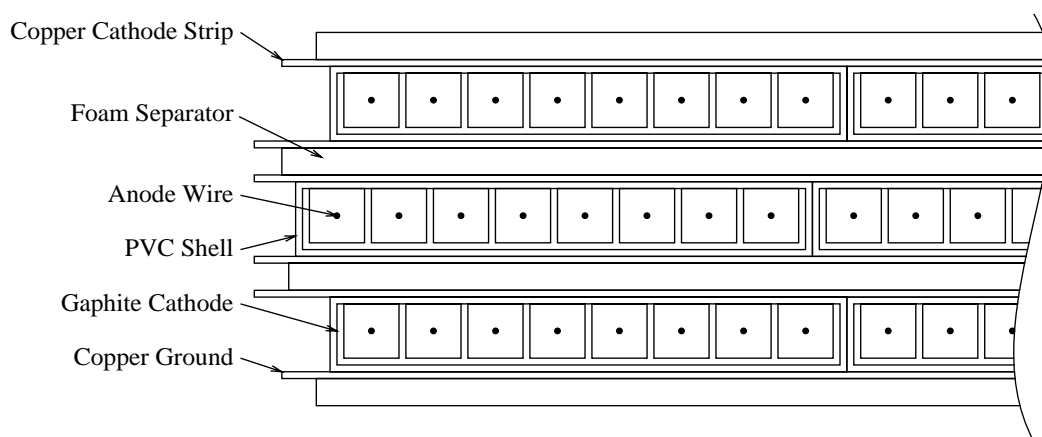


Figure 3.13: Cross Section of Superlayer Chamber in Muon Detector

need to pass all three triggers to be written onto disk. Later, after further filtering in offline software, information on disk will be stored into magnetic tape for later physics analysis.

Different levels of the trigger use different criteria. The following is the detector information used by each level:

1. L0: use TF, VD and CC.
2. L1: after L0, use VD, DR, TF, CC.
3. L2: after L1, use DR and VD.
4. L3: on-line software for disk to tape writing.

L0 trigger is the first and the fastest trigger. L0 trigger accepts information from TF, VD and CC to select events. L0 trigger attempts to reduce 2.7 MHz crossing frequency to a rate on the order of 20 kHz.

After L0 trigger, all detector gating is disabled, and a search is made for an L1 trigger requirement. L1 uses information from CD, CC and TF for events which passed the L0 trigger. It takes about  $1.0 \mu$  second for an event to arrive at L1 circuitry, causing about 2% dead time after the L0 trigger fires. If L1 is not satisfied, the system is reset and detector gating resumes. The goal of the L1 trigger is to reduce the event rate to about 25-50 Hz.

L2 trigger uses information from DR and VD to evaluate incoming events after an L1 trigger is fired. It takes about 50 times longer than L1 trigger to write an event,  $50 \mu$  seconds. L2 typically fired at about 10-20 Hz, depending on CESR conditions. When L2 trigger fired, CLEO-II data acquisition system writes out all the information gathered from the various detector components to disk. Further filtering will be employed with software L3, when information are dumping from disk to tape.

L3 is the software to further discard some unwanted events for tape storage. For example, only a pre-determined percentage of bhabha events will be written to magnetic tape. Another job L3 trigger does is to kill the “beam wall” event, which is about 45% of the events passed L2 trigger. A percentage of “random trigger” events is also kept in order to check that what the trigger has thrown away is really uninteresting.

### 3.2.8 Monte Carlo

CLEO II Monte Carlo is the simulation of  $\Upsilon(4S)$  events for the CLEO II detector environment. We use Monte Carlo to study the signal efficiency, the systematic error checks, and to estimate the backgrounds in our analysis of data.

CLEO-II Monte Carlo contains two parts:

- QQ: for physics simulation.
- CLEOG: for detector simulation.

QQ is based on our current understanding of particle physics. The program QQ generates particles produced in  $e^+e^-$  annihilations, then decays them according to several routines embedded within QQ to subsequent modes. The QQ is constantly tuned to match our current understanding of particle physics.

The decay history of each event is then passed through a program called CLEOG, based on GEANT from CERN. CLEOG simulates the complete detector response to the event. Those particles which are not decayed within QQ are handled here, such as decays in flight of  $\mu$  and  $K$ . All manner of detailed processes are simulated in CLEOG in order to make the simulated data match the true data as accurate as possible. The program simulates the energy loss of the particles while passing through the matter of the detector, the electromagnetic showering within the calorimeter, and the ionization of the drift chamber gas. Random

noise hits in the various detectors are modeled by adding hits from randomly triggered events in data.